Influence of Process Parameters and Metallic Binders on Physicomechanical and Tribological Properties of WC-based Alloys Fabricated by the SPS

Sajjad Jameel Ibrahim Al Safawee, Ali Rasooli*, Taher Rabizadeh

Department of Materials Engineering, Faculty of Mechanical Engineering, University of Tabriz, Tabriz, Iran.

*Corresponding author: Dr. Ali Rasooli (Email: a.rasooli@tabrizu.ac.ir)

Abstract

There is a global need to develop engineering materials to address the increasing demands in various industries. Spark plasma sintering (SPS) is one of the most distinguished powder metallurgy techniques, offering the opportunity for the fabrication of different types of materials. This work emphasizes optimizations of the important process parameters, including temperature, pressure, and holding time, involved in the SPS of the WC, WC-Co, and WC-Cr, as well as assessing the influence of the content of the Co (6-24 wt.%) and Cr (0.2-1 wt.%) binders on the overall characteristics of the SPS-ed cermets. The results illustrate that the process parameters highly affect the physicomechanical properties of the SPS-ed WC, where the most appropriate conditions from a physicomechanical viewpoint are obtained at a sintering temperature of 1700 °C, a pressure of 80 MPa, and a holding time of 5 min. The included Co binder reduces the optimum temperature and pressure down to 1200 °C and 70 MPa, respectively. The addition of the Co improves the final properties of the WC irrespective of its content. The highest tribomechanical properties are attained when 18 wt. % of Co is added. Similar to that of Co, the incorporation of

[DOI: 10.22068/ijmse.4597]

Cr into the WC increases the tribomechanical performance. In general, the use of Co and Cr metallic binders seems a useful strategy to promote the overall properties of the SPS-ed WC.

Keywords: WC-Co; WC-Cr; Spark Plasma Sintering; Physicomechanical properties; Tribology.

1. Introduction

Sintering is a process in which the powdered material, including ceramics, metals, etc., is compressed into a predefined shape having desired properties by the application of pressure and temperature. The latter is usually below the melting point of the primary materials. A variety of factors, including temperature, atmosphere, heating rate, pressure, and features of the primary material, are effective in determining the final properties of the final product. The main sintering methods fall under two major groups, namely pressureless sintering and pressure sintering [1-5].

The SPS technique is one of the recently-developed powder metallurgy technologies that is capable of applying heat and uniaxial pressure at the same time. This feature distinguishes the SPS from conventional powder metallurgy techniques, such as hot pressing. Unlike most conventional routes, there is no need to apply post-heat treatments at high temperatures for prolonged durations when the SPS is used [6-10]. The advantages of SPS are not limited to those mentioned above. The high heating rate, low condensation temperature, and shorter holding time of this approach lead to the fabrication of high-density products and make it possible to process materials that have poor sinterability, e.g., metals and ceramics. The technique allows to fabricate a broad variety of materials, including metals, ceramics, cermets, intermetallics, and composites [11-16].

The tungsten carbide (WC) is a ceramic compound consisting of equal numbers of tungsten and carbon atoms. The compound offers a high melting point, extraordinary hardness, low friction,

[DOI: 10.22068/ijmse.4597]

chemical and thermal stability, electrical conductivity, and resistance to corrosion and oxidation. Thanks to its excellent versatile properties, WC is employed in various harsh engineering applications, including cutting tools, mining tools, drilling equipment, and different wear- and corrosion-resistant parts [17-21]. However, the main limitations of the WC, namely poor fracture toughness, impact resistance, and plasticity, cause challenges in the use of this ceramic in long-term engineering applications. There are several strategies proposed to overcome this problem. The addition of a metallic binder phase, e.g., Co, Fe, Cr and Ni, to the WC matrix seems a reasonable solution, since in such a cermet system, the ceramic phase puts forward the hardness and wear resistance, while the metallic binder contributes to the improved ductility and fracture toughness of the product. It should be mentioned that the use of the metallic binder has its own technical problems and environmental risks. For instance, the included Co results in a drop in the hardness of the cermet and causes toxicity to the environment. Thus, precise control should be provided on the content of the added binder phase and operating factors to diminish the technical challenges and health concerns. The Cr content range (0.2–1 wt.%) in this work was designed to systematically evaluate its effectiveness as a grain growth inhibitor and microstructural modifier in WC–Co composites while maintaining Co as the dominant load-bearing binder phase [22-30].

In order to tackle the abovementioned shortcomings associated with the SPS of the WC ceramic, a comprehensive and systematic study is carried out to optimize the chief operational parameters, including sintering temperature, pressure, and holding time, involved in the SPS of the WC, WC-Co, and WC-Cr, as well as evaluating the role of the content of the Co (6-18 wt.%) and Cr (0.2-1 wt.%) binders in governing the final performance of the cermet systems. This work can be considered novel since it compares the effects of different metallic binders, their content, and SPS key process parameters on the final properties of the parts. The results of this competitive study

[DOI: 10.22068/ijmse.4597]

can open up new horizons in the selection of the most appropriate binder phase to improve the performance of the SPS-ed WC.

2. Materials and methods

2.1. Primary materials and SPS process

The primary WC, Co, and Cr powders with a size below 10 μm and a purity >90% were purchased from commercial companies. The SEM images of the powders are indicated in Fig. 1. The morphology of the WC powders is nodular and spherical. While Co powders are rounded in shape, the Cr powders show polyhedral morphology.

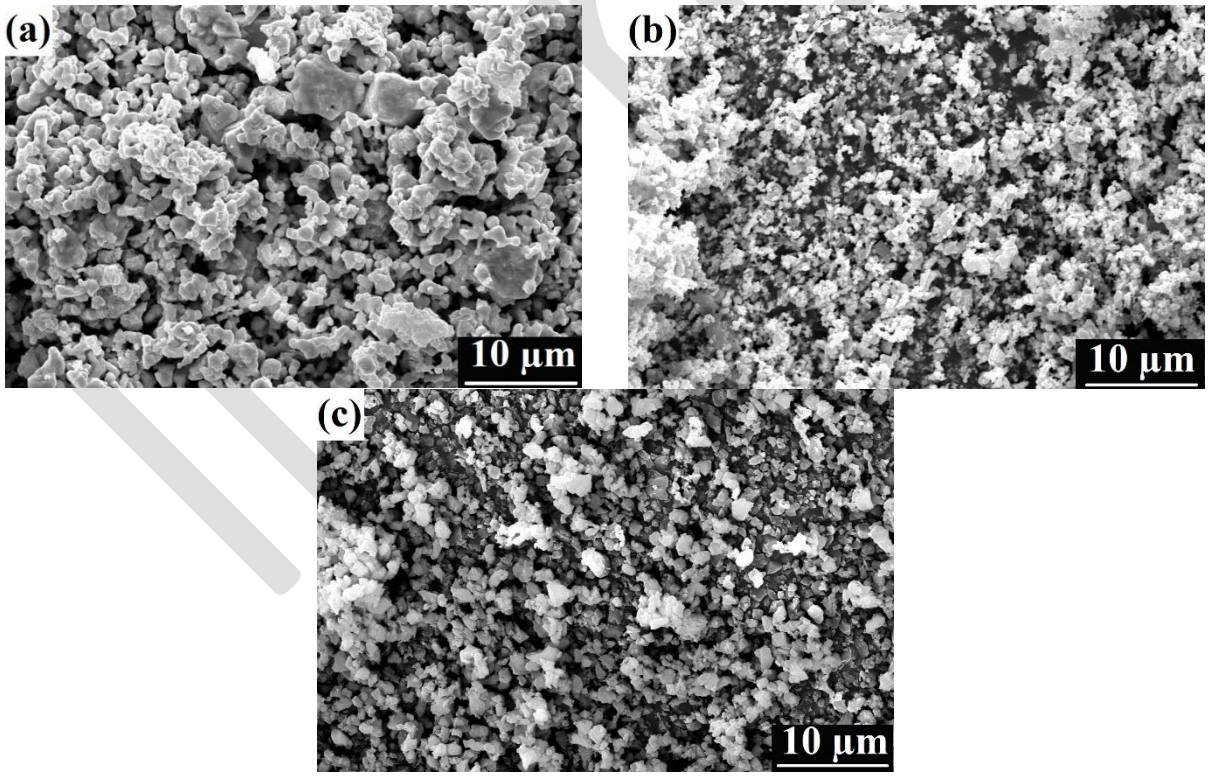

Fig. 1. SEM images of the primary powders: (a) WC, (b) Co, and (c) Cr.

[DOI: 10.22068/ijmse.4597]

The mixing process of the primary powders, i.e., WC-Co (6-24 wt.%) and WC-Cr (0.2-1 wt.%), was performed in a planetary ball mill (Faragir Sanat Mehrbin, Iran) at 300 rpm for 10 h. The ball-to-powder ratio was 10:1. In order to avoid oxidation of the Co and Cr, and reduce the risk of contamination, the ball milling process was done under the argon atmosphere.

An SPS apparatus (Electrooptic Co., Iran) was employed to sinter the powders. The diameter and thickness of the disk-shaped SPS-ed parts were 30 mm and 3 mm, respectively. The SPS was performed under DC condition and argon atmosphere. In order to optimize the process parameters, the WC, WC-Co, and WC-Cr samples were SPS-ed under various conditions, outlined in Table 1. Moreover, a schematic demonstration of the ball milling and SPS processes applied in the present work is provided in Fig. 2.

Table 1. The SPS conditions applied to fabricating WC, WC-Co, and WC-Cr samples.

Specimen	Voltage (V)	Heating rate (°C/min)	Pressure (MPa)	Temperature (°C)	Holding time (min)
WC	8	100	20-80	1600-1700	5-15
WC-Co	8	100	30-70	1100-1200	5
WC-Cr	8	100	30-70	1400-1600	5

[DOI: 10.22068/ijmse.4597]

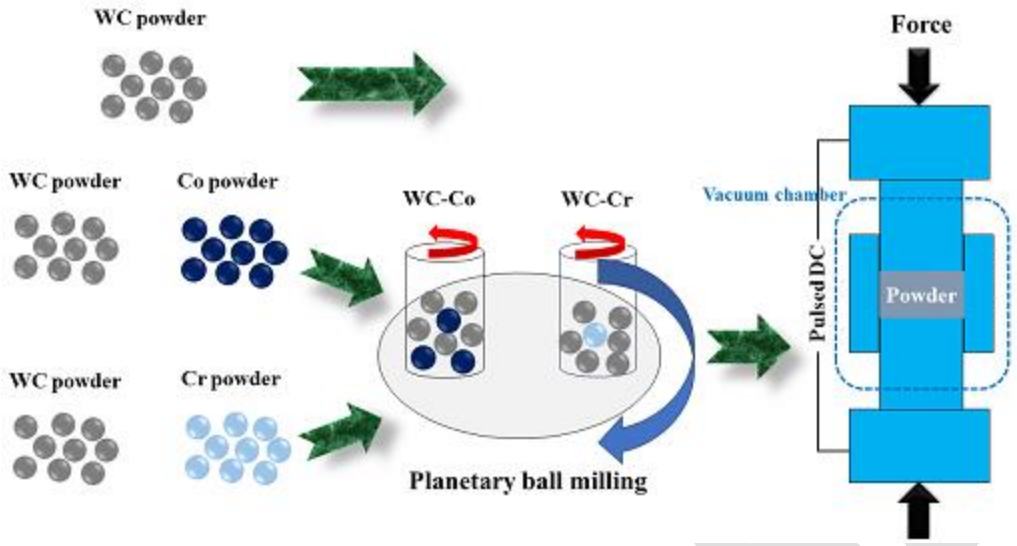

Fig. 2. A schematic demonstration of the ball milling and SPS processes applied in the present work.

2.2. Characterization

The phase composition of specimens was determined using X-ray diffraction (XRD; Tongda-TD3700, China) by the Cu-Kα radiation source over the 2θ range of 10-80º at a step size of 0.02º.

The bulk density of the specimens was calculated using the Archimedes method according to the ASTM C 373-88 standard [31].

A microhardness tester (Emco test, M4U-250, Austria) was used to measure the microhardness of the specimens at a load of 100 g for a dwelling time of 10 s. The test was done on five different parts of the specimens and mean results were reported.

The tensile mechanical properties of the specimens were studied by uniaxial tensile testing (Houns Field, H50KS, UK) in accordance with the ASTM: E8/8 M standard [32]. The cross-head speed

[DOI: 10.22068/ijmse.4597]

during the tensile test was 1 mm/min. The bending properties of the specimens were evaluated by a universal testing machine (SANTAM, STM-150, Iran).

A pin-on-disk tribometer (Tajhiz Sanat Nasr, Iran) consisting of a WC pin was utilized to determine the tribological properties of the specimens at a temperature of 25±2 °C and a humidity of 45%. The applied load, sliding distance, and sliding speed were 30 N, 200 m, and 120 rpm, respectively.

Scanning electron microscopy (SEM; Philips, XI30, the Netherlands) was employed to observe the morphology of the fracture and worn surfaces.

3. Results and discussion

3.1. Physicomechanical properties of SPS-ed WC

As mentioned earlier, the sintering temperature, pressure and holding time are of chief importance in governing the final properties of the SPS-ed specimens. Thus, these parameters should be optimized to boost the efficiency and performance of the SPS-ed part. Table 2, Table 3, and Table 4 outline the physicomechanical properties of the SPS-ed WC specimen at various sintering temperatures (1600-1700 °C), pressures (20-80 MPa), and holding times (5-15 min), respectively.

Table 2. Physicomechanical properties of the WC specimens SPS-ed at various sintering temperatures.

Temperature (°C)	**Pressure (MPa)**	**Bulk density (g/cm^3)**	**Microhardness (HV)**	**Tensile strength (MPa)**
1600	40	10.6	1436	418
1650	40	11.2	1573	435

[DOI: 10.22068/ijmse.4597]

1700	40	12.1	1825	460

Table 3. Physicomechanical properties of the WC specimens SPS-ed at various sintering pressures.

Temperature (°C)	Pressure (MPa)	Bulk density (g/cm^3)	Microhardness (HV)	Tensile strength (MPa)
1700	20	10.1	1640	386
1700	40	12.1	1825	460
1700	60	12.9	1911	509
1700	80	13.5	2034	524

Table 4. Physicomechanical properties of the WC specimens SPS-ed at various holding times.

Temperature (°C)	Pressure (MPa)	Holding time (min)	Bulk density (g/cm^3)	Microhardness (HV)	Tensile strength (MPa)
1700	80	5	13.5	2034	524
1700	80	10	12.4	1969	412
1700	80	15	11.7	1890	374

The results outlined in Table 2 show that the highest physicomechanical properties are obtained when the sintering temperature is increased up to 1700 °C. A potential mechanism leading to an increased performance at the elevated sintering temperatures can be attributed to higher

[DOI: 10.22068/ijmse.4597]

connections between the powders, i.e., decreased porosity, due to the accelerated growth rate at such temperatures. Moreover, better necking might be formed between the powders at elevated temperatures. There is a direct relationship between increased sintering pressure and higher physicomechanical performance of the SPS-ed specimens (see Table 3). A higher pressure can result in a diminished space between the powders, as well as enhanced diffusion during the sintering process. It is obvious that the dense specimens show stronger mechanical performance. On the other hand, the prolonged holding time inversely affects the physicomechanical behavior of the specimens, possibly owing to the excessive grain growth, oxidation, and thermal stresses. According to the results shown in Table 4, the application of the SPS technique leads to achieving desirable densification in the short duration. The SEM fractography of the WC specimen SPS-ed under the optimum conditions is presented in Fig. 3. The image clearly shows the brittle intergranular fracture that occurred.

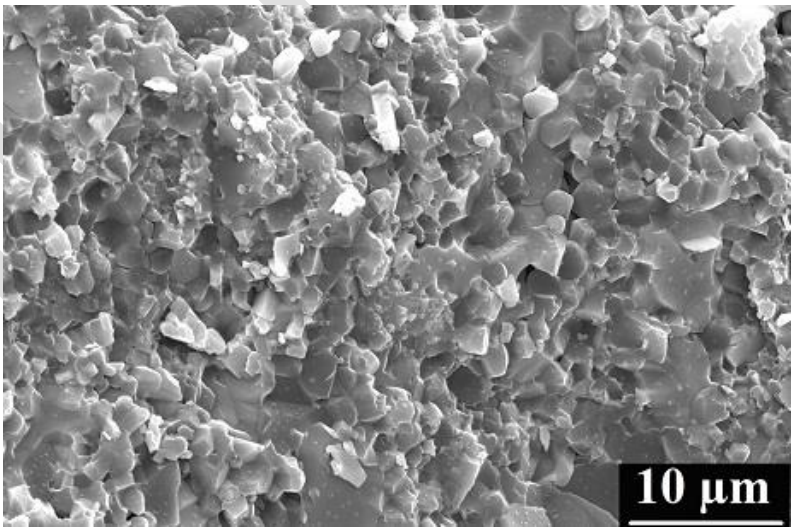

Fig. 3. SEM fractography of the WC specimen SPS-ed under the optimum conditions, i.e., temperature of 1700 °C, pressure of 80 MPa, and holding time of 5 min.

[DOI: 10.22068/ijmse.4597]

Fig. 4 indicates the coefficient of friction (COF)-distance curve of the WC fabricated under the optimum SPS conditions, along with the SEM images of the worn surface at different magnifications. The wear-induced weight loss and mean COF values were 12.4 mg and 0.61, respectively. Fig. 4a) shows that the COF variation is relatively steady along the sliding distance. There are several cracks and delamination all over the wear track, as shown by the arrows in Fig. 4c). The dominant wear mechanism is delamination.

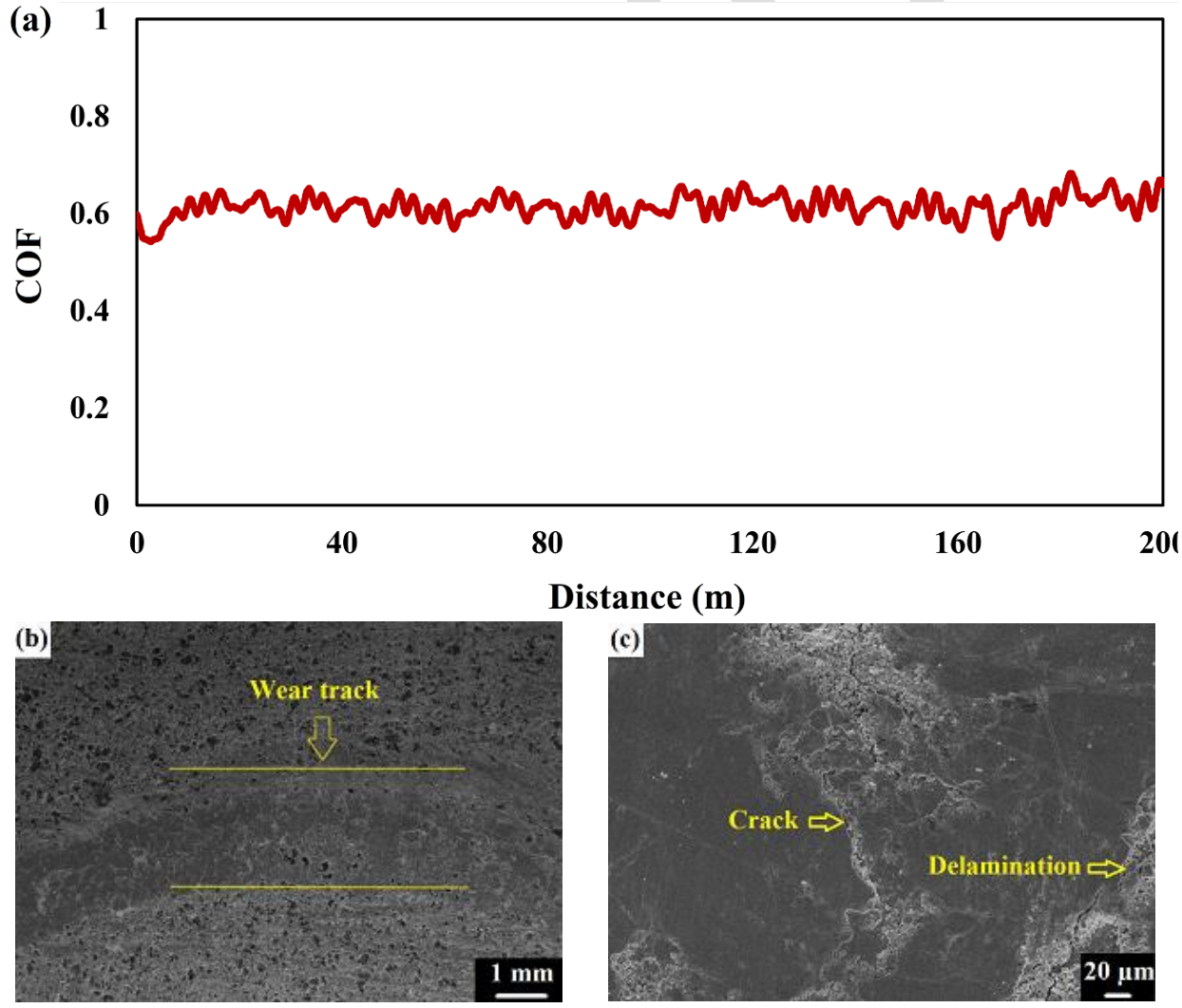

[DOI: 10.22068/ijmse.4597]

Fig. 4. (a) COF-distance curve of the WC fabricated under the optimum SPS conditions and (b,c) SEM images of the worn surface at different magnifications.

3.2. Physicomechanical properties of SPS-ed WC-Co and WC-Cr cermets

3.2.1. Effect of process parameters

In order to obtain the appropriate process parameters from a physicomechanical viewpoint, the overall properties of the WC-18 wt.% Co and WC-1 wt.% Cr SPS-ed under different sintering temperatures and pressures were evaluated. Table 5 lists the physicomechanical properties of the WC-18 wt.% Co and WC-1 wt.% Cr SPS-ed under temperature ranges of 1100-1200 °C and 1400-1600 °C, respectively.

Table 5. The physicomechanical properties of the WC-18 wt.% Co and WC-1 wt.% Cr SPS-ed under different temperature ranges. The holding time was kept constant at 5 min.

WC-18 wt.% Co				
Temperature (°C)	**Pressure (MPa)**	**Bulk density (g/cm^3)**	**Microhardness (HV)**	**Tensile strength (MPa)**
1100	70	15.8	1740	1058
1150	70	16.1	1783	1094
1200	70	16.6	1852	1132
WC-1 wt.% Cr				
Temperature (°C)	**Pressure (MPa)**	**Bulk density (g/cm^3)**	**Microhardness (HV)**	**Tensile strength (MPa)**

[DOI: 10.22068/ijmse.4597]

1400	70	12.9	1755	962
1500	70	13.4	1831	1018
1600	70	13.9	1868	1085

The physicomechanical properties of the WC-18 wt.% Co and WC-1 wt.% Cr SPS-ed under the pressure range of 30-70 MPa are illustrated in Table 6.

Table 6. The physicomechanical properties of the WC-18 wt.% Co and WC-1 wt.% Cr SPS-ed under pressure range of 30-70 MPa. The holding time was kept constant at 5 min.

WC-18 wt.% Co				
Temperature (°C)	**Pressure (MPa)**	**Bulk density (g/cm^3)**	**Microhardness (HV)**	**Tensile strength (MPa)**
1200	30	15.1	1686	1033
1200	50	15.9	1744	1075
1200	70	16.6	1852	1132
WC-1 wt.% Cr				
Temperature (°C)	**Pressure (MPa)**	**Bulk density (g/cm^3)**	**Microhardness (HV)**	**Tensile strength (MPa)**
1600	30	12.6	1710	958
1600	50	13.1	1793	1029

[DOI: 10.22068/ijmse.4597]

1600	70	13.9	1868	1085

The first notable point from the abovementioned results is the low sintering temperature range used for SPS of the cermets, especially for the WC-Co cermet, which is 500 °C lower than that of WC. This behavior can be attributed to the presence of Co binder, at high content, in the structure of the cermet. Similarly, a decrease, not as much as that was obtained for Co, in the sintering temperature is observed with the included Cr. However, at the same sintering temperature, i.e., 1600 °C, and even lower sintering pressure, there is a %20 increase in the bulk density of WC with the addition of 1 wt. % Cr. This confirms the role of the Cr as a suitable binder.

Similar to the results obtained for SPS-ed WC, the increase in sintering temperature and pressure leads to higher physicomechanical behavior in both cermets. In summary, the most appropriate sintering temperatures for WC-Co and WC-Cr cermets are 1200 °C and 1600 °C, respectively. Regarding sintering pressure, both cermets showed fruitful performance when a pressure of 70 MPa was applied.

A comparison between the physicomechanical properties of the cermets SPS-ed under optimum conditions with those of optimized WC shows the higher bulk density and tensile strength of the cermets compared to the WC, while the SPS-ed WC has a higher microhardness than that of cermets. The higher microhardness of WC-1wt.% Cr than WC-18 wt.% Co relates to the lower amount of the binder and higher intrinsic hardness of Cr. This inversely affects the tensile strength of the produced cermets, where WC-18 wt.% Co shows higher tensile strength, which is a marker of their superior toughness.

[DOI: 10.22068/ijmse.4597]

3.2.2. Effect of Co and Cr contents

Fig. 5 illustrates the XRD diffractograms of the SPS-ed specimens containing different amounts of Co and Cr binders.

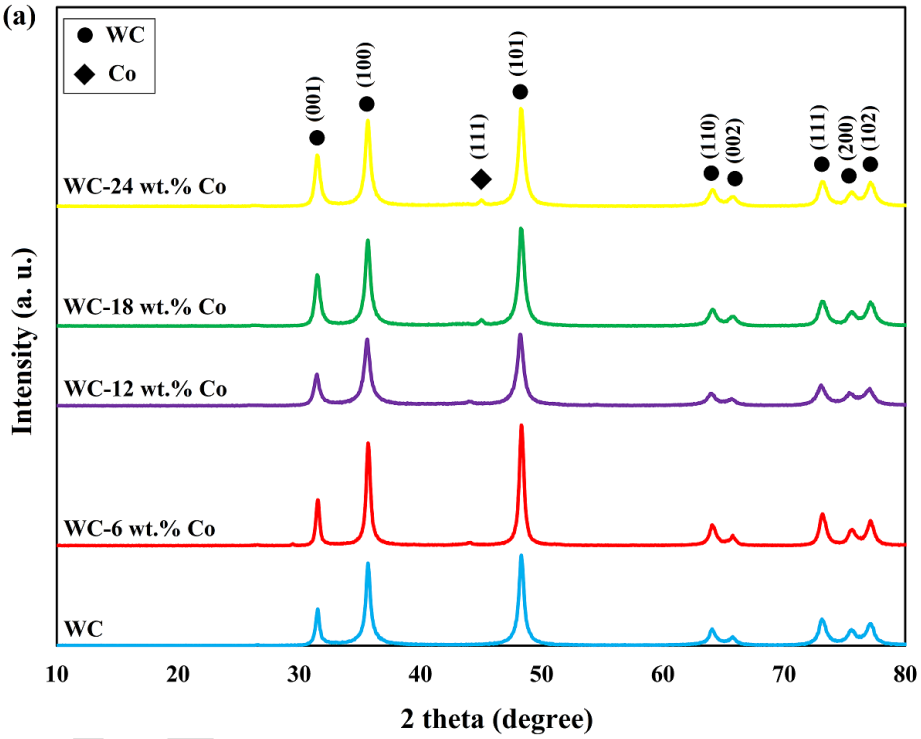

[DOI: 10.22068/ijmse.4597]

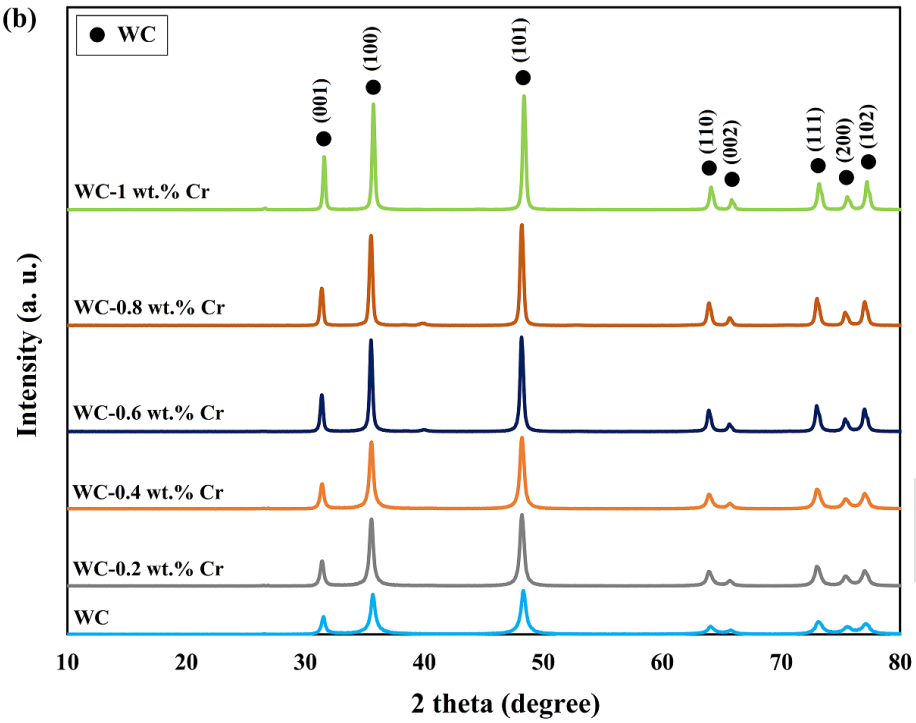

Fig. 5. XRD diffractograms of the SPS-ed specimens (a) WC- different amounts of Co and (b) WC- different amounts of Cr.

The XRD diffractograms in Fig. 5a) show that the phase structure of the SPS-ed WC is merely composed of WC peaks appearing at 2Θ ≈ 31°, 35°, 48°, 64°, 65°, 73°, 75°, and 77°. A low-intensity α-Co peak at 2Θ ≈ 44° with a face-centered-cubic (FCC) crystal structure emerged in the diffractograms of the WC-Co cermets. There exists a possibility of forming the C-poor W_2C phase and η-phase (W_3Co_3C or W_6Co_6C) during the WC-Co cermet sintering. The mentioned phases show very low plasticity and poorly wet WC. Hence, the possible formation of these compounds can drastically degrade the final performance of the cermet. The lack of these phases in the phase composition of the SPS-ed WC-Co cermet in this work is desired from a tribomechanical point of view. On the other hand, it is theoretically established that α-Co is stable at high temperatures,

[DOI: 10.22068/ijmse.4597]

where the ε-Co to α-Co phase transformation occurs at 417 °C. The reason why α-Co phase presents in the phase structure of the cermets at room temperature, can be attributed to dissolution of W and C in α-Co during the SPS process, which resulted in a stability of α-Co at room temperature. The formation of the α-Co phase can greatly contribute to the enhanced mechanical properties, since it offers superior fracture toughness than that of ε-Co [33, 34].

The diffractograms indicated in Fig. 5b) illustrate that there is no significant change in the phase composition of the WC with the inclusion of the Cr. The lack of the Cr peak in the diffractograms of the WC-Cr cermets is ascribed to the low amount of Cr in their microstructure, which is below the detection limit of the XRD.

Another notable point from the diffractograms is that there are no new WC peaks appearing or no one disappears when the binders are added to the WC. Moreover, there is no change in the main growth orientation of the WC crystals, so that the crystals are most likely to grow along (101) planes in all specimens.

The changes in the bulk density of the WC-Co and WC-Cr cermets as a function of binder's content in the cermet are indicated in Fig. 6. In WC-Co cermet, a slight increase in bulk density is observed with an increased amount of Co over the 6-12 wt.% range, followed by a sharp enhancement with a further increase in Co content up to 18 wt.%. A further rise in the Co content up to 24 wt.% has an insignificant influence on the bulk density of the cermet. The bulk density of the WC-Cr cermet is continuously increased with the increased Cr content from 0.2 to 1 wt.%.

[DOI: 10.22068/ijmse.4597]

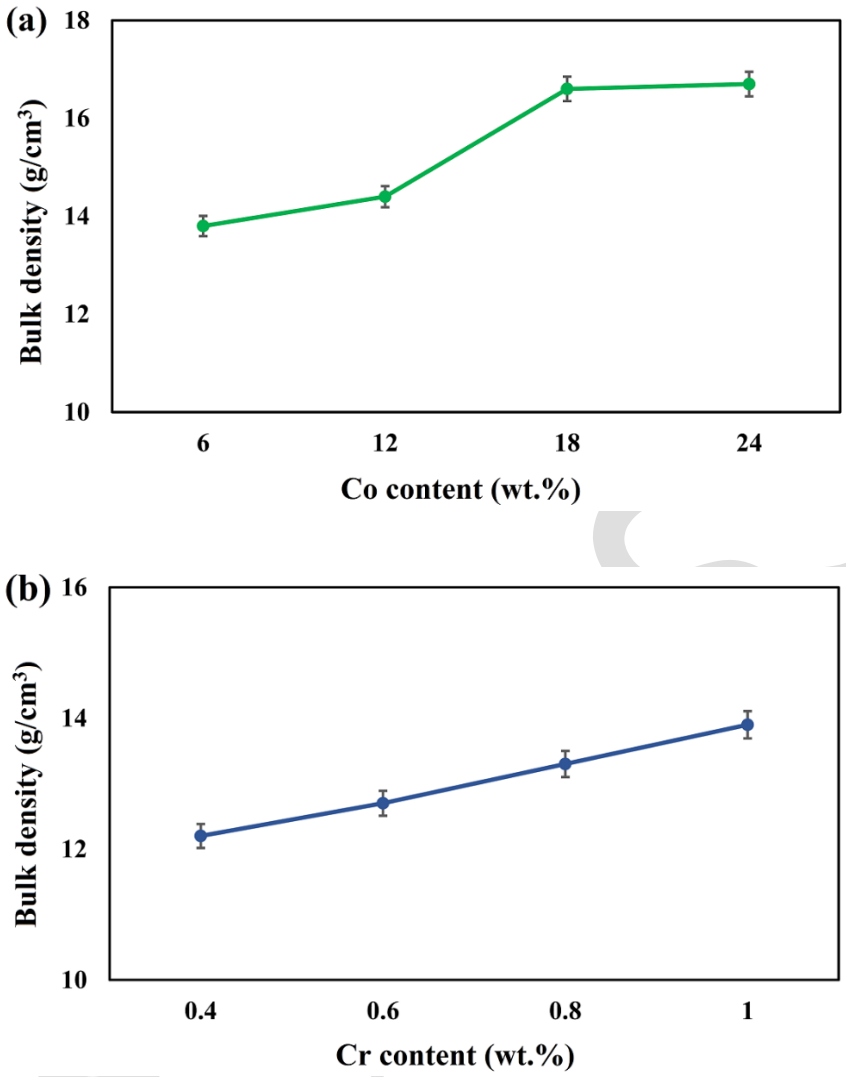

Fig. 6. Changes in the bulk density of the WC-Co and WC-Cr cermets as a function of binder's content in the cermet: (a) WC-Co and (b) WC-Cr.

There are three parameters leading to an increase in bulk density of the WC with the added Co and Cr binders, as follows: (i) *liquid phase sintering*; since the melting point of the WC is much higher than that of Co and Cr, the solid binders are transformed into liquid phase during the SPS. The liquid phase is beneficial for improved densification and grain bonding since it can easily diffuse

[DOI: 10.22068/ijmse.4597]

through the existing spaces and voids between the WC particles via capillarity to reduce the porosity. The liquid Co or Cr phase can also facilitate the mass transfer between the particles, leading to an enhanced density; (ii) *Grain bonding*; the Co and Cr binders can efficiently wet the surface of the WC particles, resulting in a stronger interface between them; and (iii) *Thermomechanical stabilization*; the high toughness and ductility of the binders, especially Co, can contribute to the enhanced density through stress redistribution. The added Co diminishes the thermal expansion mismatch between the WC particles during the cooling stage, leading to a decreased internal stress and less void formation. In SPS, besides conventional liquid-phase-assisted densification, the added binder plays a key role in determining the electrical and thermal characteristics of the powder compact. The included binder increases interparticle electrical conductivity through enhancing particle–particle contact and decreasing contact resistance during the early stages of sintering; Therefore, facilitates the formation of continuous current pathways within the part. Consequently, localized temperature gradients at particle interfaces are increased, leading to accelerated diffusion, neck formation, and particle rearrangement even under the short dwell times characteristic of SPS [35-38].

The performance and durability of an engineering part depends heavily on its mechanical properties, e.g., hardness, strength, and toughness. Fig. 7 shows the microhardness of the SPS-ed WC-Co and WC-Cr cermets containing various amounts of the metallic binders. The microhardness of the both fabricated cermets is lower than that of WC due to the softer nature of the Co and Cr elements. The higher hardness of the Cr compared to the Co, as well as its lower content in the cermet, lead to the enhanced microhardness of the WC-Cr specimens [39]. A general decreasing trend is seen in the microhardness of the cermets with the increased content of metallic binders.

[DOI: 10.22068/ijmse.4597]

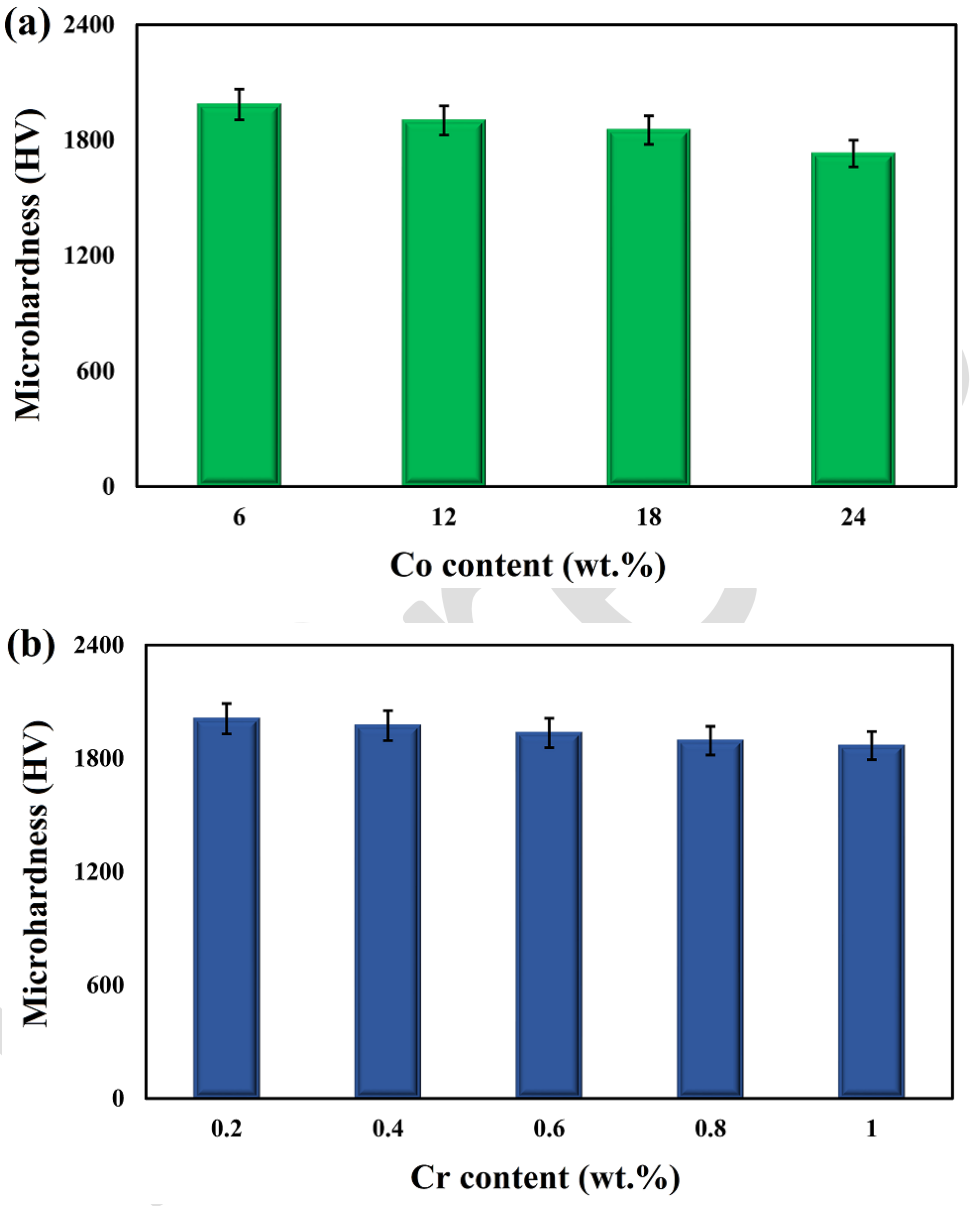

Fig. 7. Microhardness of the SPS-ed (a) WC-Co and (b) WC-Cr cermets containing various amounts of the metallic binders.

The tensile strength values of the cermets consisting of various binder contents are indicated in Fig. 8. The results show that the increased Co and Cr contents significantly contributes to the

[DOI: 10.22068/ijmse.4597]

enhanced tensile strength of the cermets. However, an increase in Co content over the 18-24 wt. % range has no role in improving the strength.

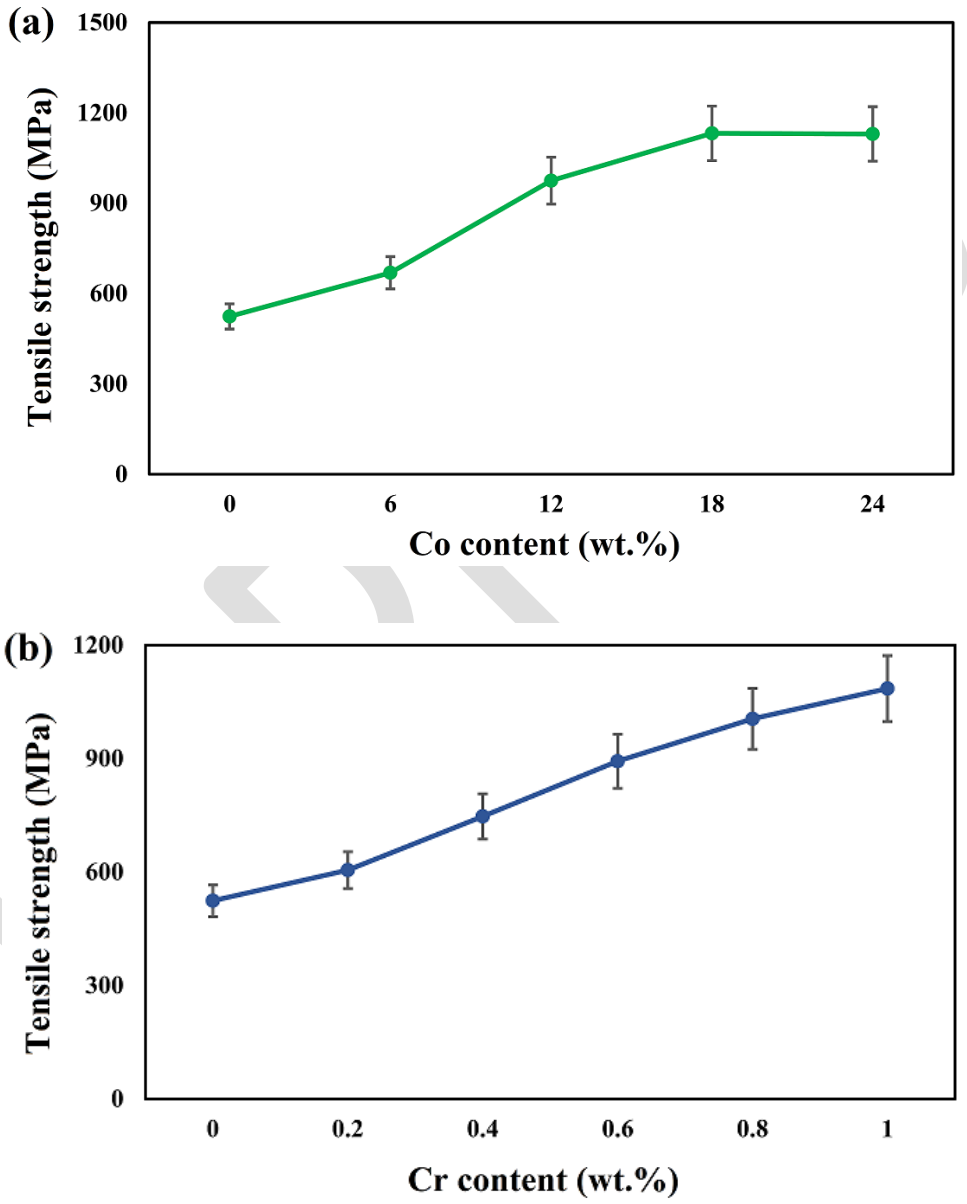

Fig. 8. Tensile strength values of the cermets consisting of various binder contents: (a) WC-Co and (b) WC-Cr.

[DOI: 10.22068/ijmse.4597]

The introduction of Co and Cr metallic binders to the brittle WC ceramic leads to a composite material, in which the WC particles are embedded in the ductile Co or Cr matrix. The formation of such a ductile matrix improves the energy absorption under tensile loading and, therefore, promotes the toughness and strength of the cermet. Moreover, as mentioned in Fig. 6, the enhanced bulk density of the cermets with the higher amounts of the binders is another potential parameter resulting in an enhanced tensile strength. The high plastic deformation capability of the binders, especially Co, leads to decreased stress concentration sites all over the specimen under the tensile loading, thereby improving the tensile strength [39, 40].

SEM fracture surface of the studied SPS-ed cermets at different magnifications are presented in Fig. 9. There are notable differences between the fracture surface of the cermets and that of WC (provided in Fig. 3). The micrographs confirm the intergranular diffusion of the binders during the SPS. As seen, the Co and Cr binders are evenly distributed throughout the WC grain boundaries, so that the higher content of the binders increases the chance of reaching full densification, since there might be higher liquid phase to fill the pores. The pores are considered the potential sites for crack initiation, which consequently results in failure. The high-magnification images illustrate the compact and uniform fracture surface containing low porosity content when high amounts of the binders are used, i.e., >12 wt.% Co and >0.8 wt. % Cr. The porous fracture surface of the cermets in Fig. 9a, a′, b′, and c′) can be related to the low amounts of the binder, where the short holding time of the process does not allow the low liquid phase to completely fill the pores. On the other hand, the use of excessive amounts of the Co binder, i.e., 24 wt. %, leads to agglomeration of the binder phase, which may degrade densification. The main fracture mechanisms in the studied cermets are intergranular and intragranular.

[DOI: 10.22068/ijmse.4597]

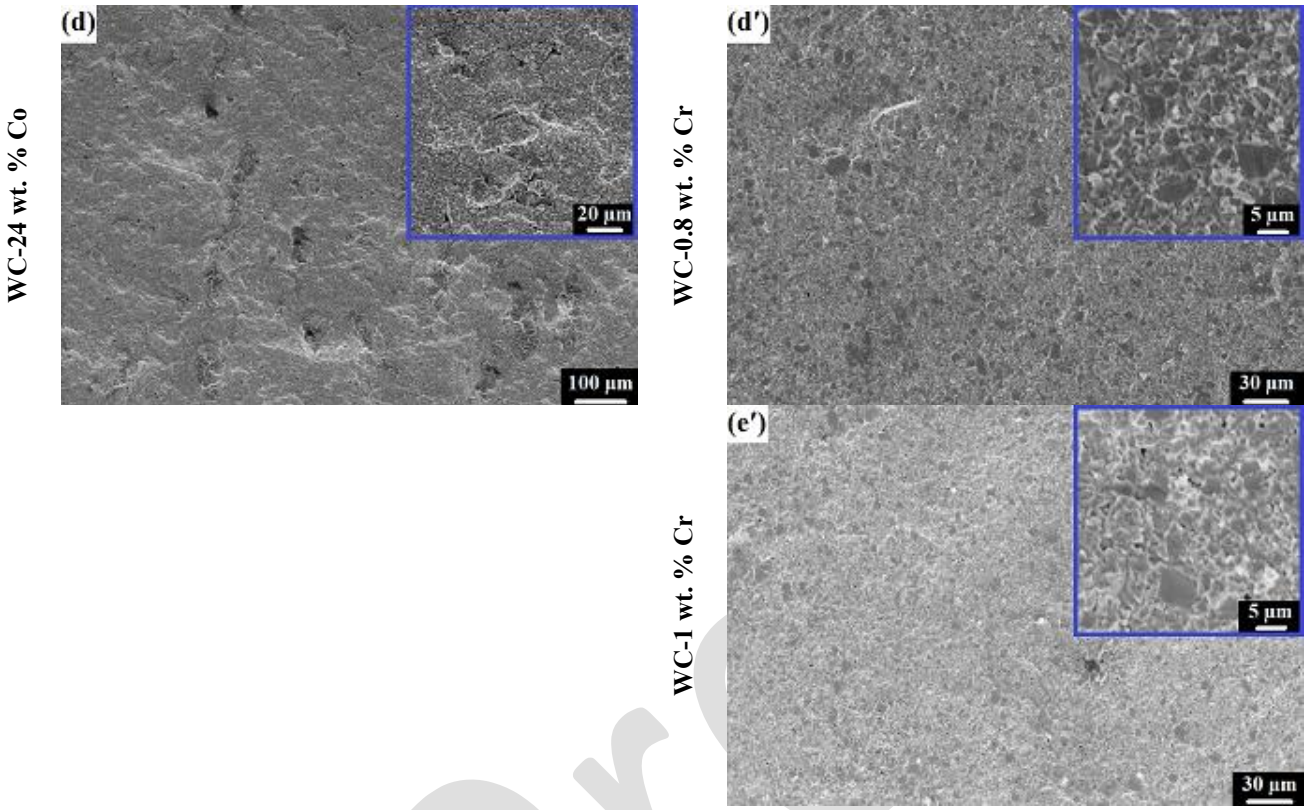

Fig. 9. SEM fracture surface of the studied SPS-ed cermets at different magnifications: (a-d) WC-Co and (a′-e′) WC-Cr.

Fig. 10 provides the bending strength values of the SPS-ed cermets containing different contents of the binders. The bending strength of the cermets is noticeably higher than that of pure WC. The higher the binder content, the higher the bending strength is. The increased ductility and toughness of the cermets as a result of the binders' inclusion, as well as the enhanced bulk density, are two main factors leading to enhanced bending strength in the WC-Co and WC-Cr cermets [26, 33].

[DOI: 10.22068/ijmse.4597]

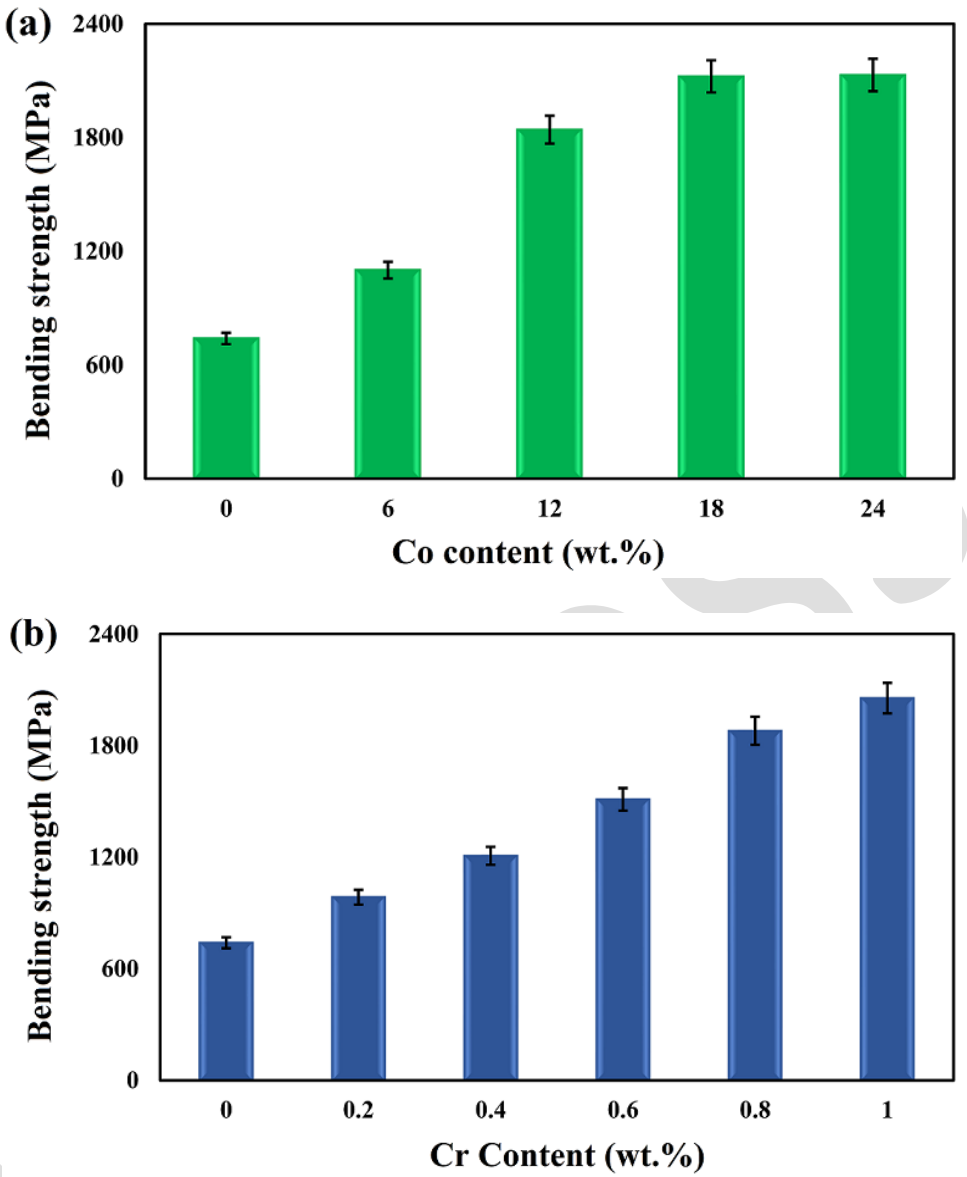

Fig. 10. Bending strength values of the SPS-ed cermets containing different contents of the binders: (a) WC-Co and (b) WC-Cr.

The COF-distance diagrams of the studied cermets are presented in Fig. 11. The mean COF and mass loss values obtained from the pin-on-disk test are listed in Table 7. The outcomes show that the average COF values are close together, demonstrating the homogenous microstructure of the SPS-ed cermets and the application of the optimum process parameters. While the increased

[DOI: 10.22068/ijmse.4597]

content of Cr leads to a continuous fall in the average COF value of the WC-Cr, the best outcome is obtained for WC-18 wt. % Co. The increase in the Co content up to 24 wt. % has no positive influence on the tribological properties of the WC-Co cermet. The decrease in mass loss correlates with the higher wear resistance of the specimen. It is concluded that the cermets containing optimum contents of the metallic binders prevent mass loss, enabling excellent wear resistance. The main factors leading to the enhanced wear resistance of the Co- and Cr-containing cermets are provided below: (i) *Improved toughness*, it was discussed earlier that the included Co and Cr binders are ductile and can improve the ductility of the cermet. The tougher the material, the higher the energy absorbed under wear test. Moreover, there is a reduced possibility for crack propagation in tough materials under mechanical stresses. On the other hand, the ductile nature of the Co and Cr may provide a solid-state lubricity at the surface/pin interface, diminishing the COF through the formation of a tribolayer; and (ii) *Providing stronger bonding between the WC grains*, the added Co and Cr binders make the WC intergranular bond stronger, which prevents the detachment of the grains, i.e., mass loss, during the wear test.

[DOI: 10.22068/ijmse.4597]

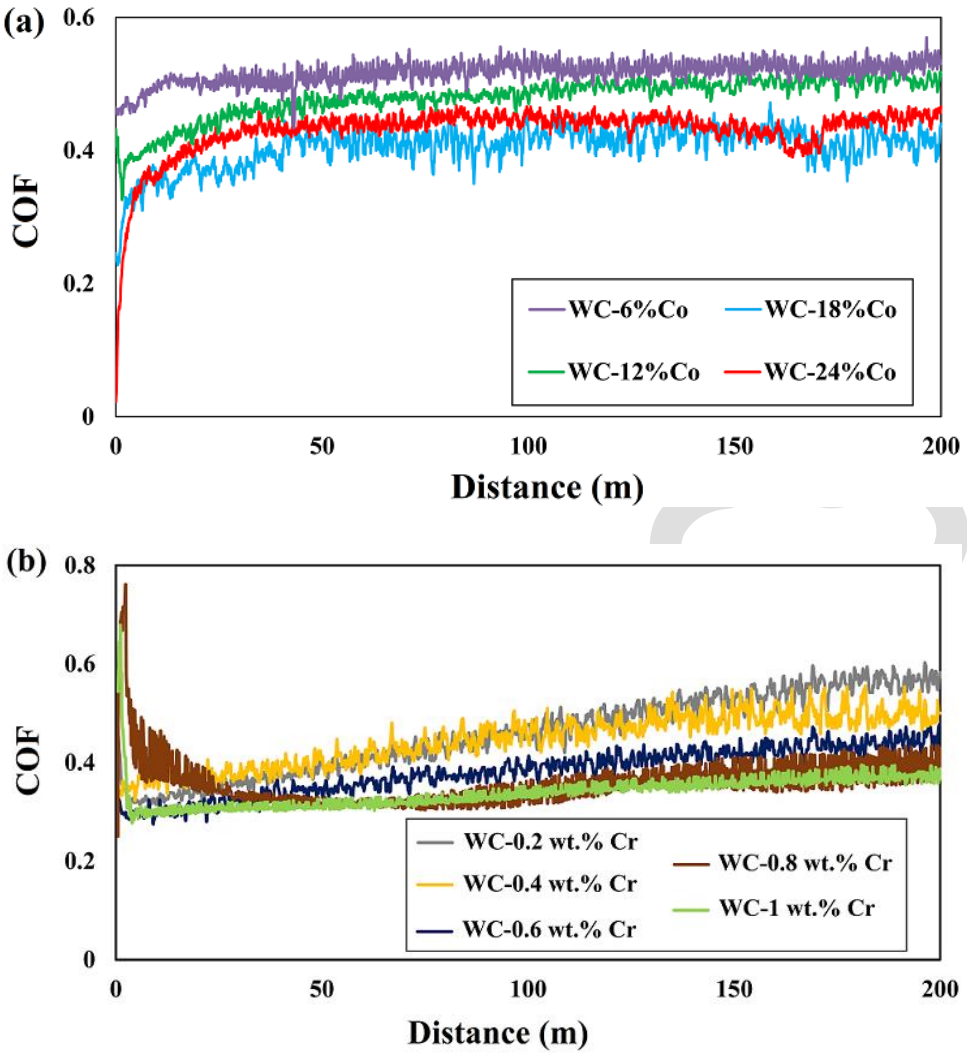

Fig. 11. COF-distance diagrams of the studied cermets: (a) WC-Co and (b) WC-Cr.

[DOI: 10.22068/ijmse.4597]

Table 7. mean COF and mass loss values of the cermets obtained from the pin-on-disk test.

WC-Co		
Binder content (wt. %)	**Mean COF**	**Mass loss (mg)**
6	0.51	5.1
12	0.47	4.5
18	0.40	1.9
24	0.42	2.7
WC-Cr		
0.2	0.48	4.9
0.4	0.45	4.1
0.6	0.43	3.2
0.8	0.40	2.6
1	0.37	1.7

The SEM images of the worn surfaces of the SPS-ed WC-Co and WC-Cr specimens are shown in Fig. 12. The images show the formation of tribolayer over the wear tracks, and there is no wear debris on the tracks. The higher the binder contents, the higher the possibility of the formation of a continuous tribolayer. The formation of tribolayer containing mixed oxides originating from W and the Co/Cr binder is probable due to their affinity to oxidation. The formed tribolayer can stabilize the tribolayer during sliding. A non-continuous tribolayer forms when a low amount of the binder is added to WC (see Fig. 12a). Furthermore, the high hardness of the WC-1 wt.% Cr

[DOI: 10.22068/ijmse.4597]

limits the contact area between the surface and pin, shown in Fig. 12 e′, resulting in low wear damage.

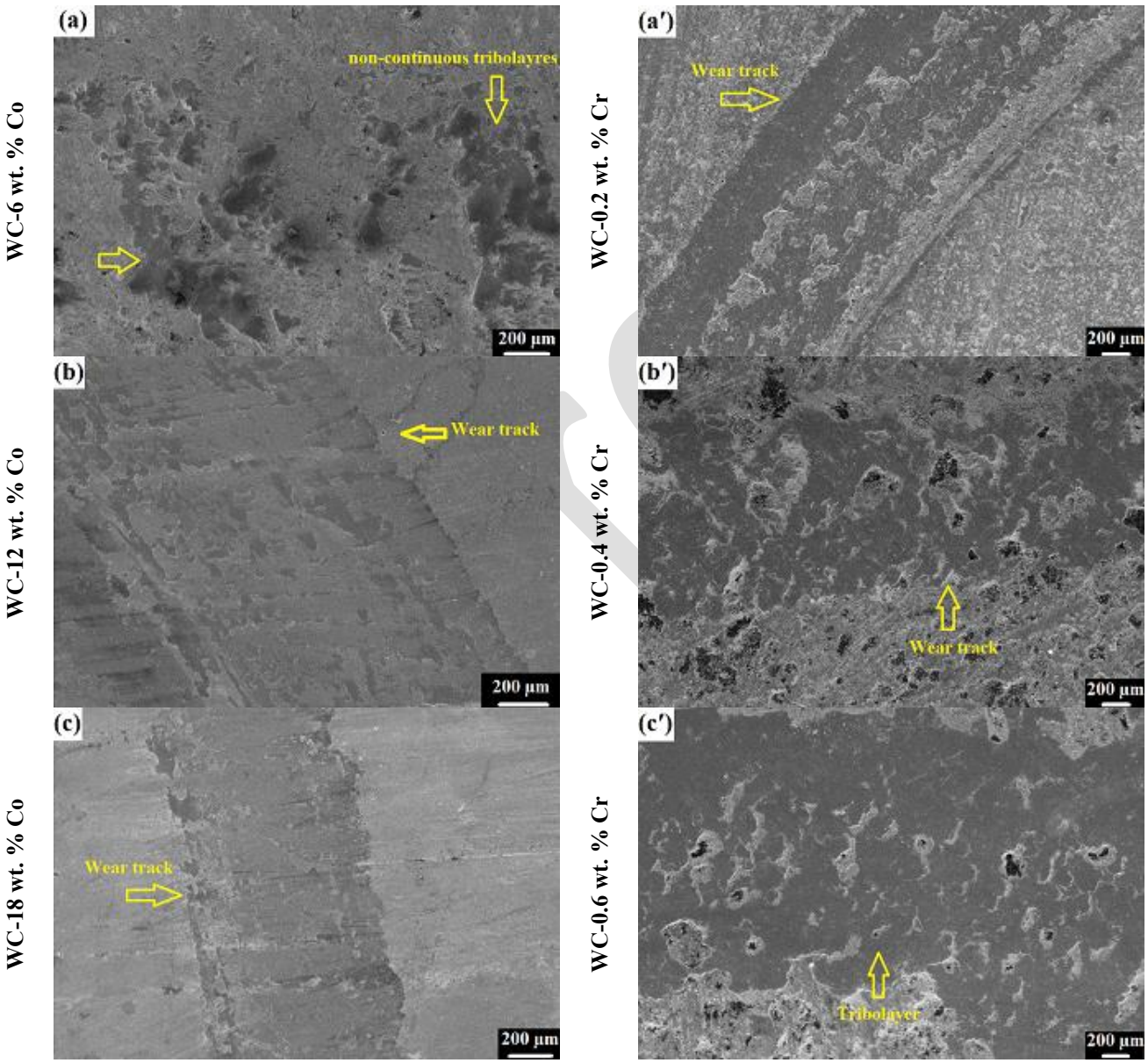

[DOI: 10.22068/ijmse.4597]

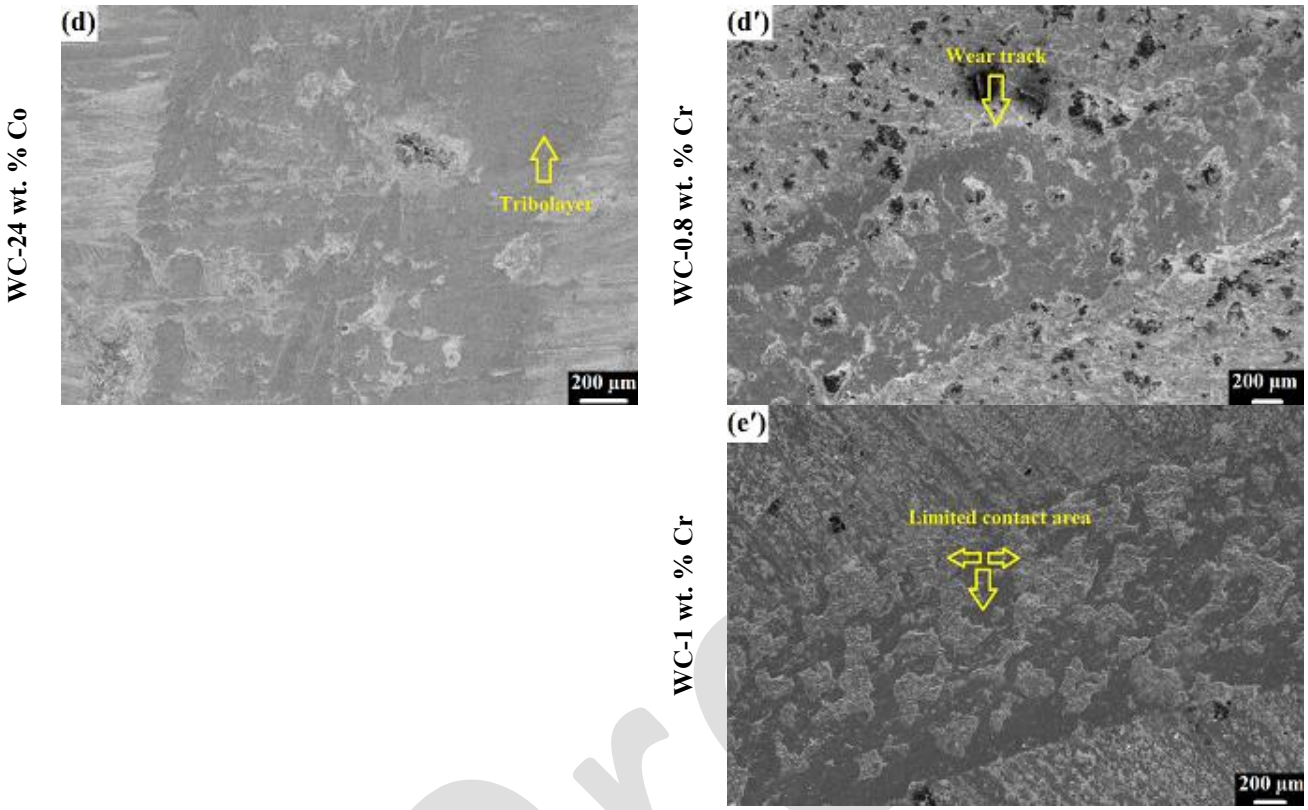

Fig. 12. SEM images of the worn surfaces of the SPS-ed (a-d) WC-Co and (a′-e′) WC-Cr specimens.

3.3. *Summary and comparative insight*

Before making a comparison between the performance of the SPS-ed WC-Co and WC-Cr cermets, it is to be noted that the applied strategy to add a metallic binder at any content leads to an improvement in the physicomechanical and tribomechanical properties of the SPS-ed WC ceramic. Both of the added metallic binders decreased the optimum sintering temperature of the WC. The decrease in optimum sintering temperature of the WC-Co is more pronounced. Although the content of the Co binder is higher than that of Cr, there is not much difference between the

[DOI: 10.22068/ijmse.4597]

microhardness of the cermets, while the bulk density and tensile strength of the WC-Co are markedly higher than those of WC-Cr. In the case of fracture mechanism and bending strength, there is no noticeable difference between the SPS-ed cermets. While both metallic binders led to the formation of a tribolayer under wear condition, the COF and mass loss of the WC-Cr cermet are lower than those of WC-Co, maybe due to the slightly higher microhardness of Cr-containing cermet according to the Archard's law [41]. Table 8 lists the obtained physicomechanical properties of the SPS-ed parts produced under optimum conditions in order to provide a comparative insight into their final performance.

Table 8. Physicomechanical properties of the SPS-ed parts produced under optimum conditions in order to provide a comparative insight into their final performance.

Sample	Bulk density (g/cm^3)	Microhardness (HV)	Tensile strength (MPa)	COF	Mass loss (mg)
WC	13.5	2034	524	0.61	12.4
WC-1Cr	13.9	1868	1085	0.37	1.7
WC-18Co	16.6	1852	1132	0.40	1.9

4. Conclusions

This work aimed to address the undesired mechanical properties of the SPS-ed WC ceramic, namely poor toughness, tensile and bending strength, which consider a potential challenge facing its engineering applications, through the addition of the various contents of Co (6-24 wt.%) and Cr (0.2-1 wt.%) metallic binders. The main results are as follows:

[DOI: 10.22068/ijmse.4597]

(i) The optimum sintering temperature, pressure, and holding time for SPS of the pure WC were 1700 °C, 80 MPa, and 5 min, respectively.

(ii) The addition of metallic binders, especially Co, reduced the sintering temperature and pressure of the SPS process to reach the optimum physicomechanical properties. The optimum sintering temperature for WC-Co and WC-Cr cermets was 1200 °C and 1600 °C, respectively.

(iii) The bulk density and tribological properties, as well as tensile and bending strength, of the SPS-ed WC are profoundly increased with the addition of the metallic binders. The increase in the Co binder content up to 18 wt.% and Cr content up to 1 wt.% led to the most desirable outcomes.

(iv) The microhardness of both cermets fabricated under optimum conditions, regardless of the binder content, was lower than that of the optimum WC. The microhardness value decreased from ≈2034 HV for WC to ≈1852 HV and ≈1868 HV for WC-Co and WC-Cr, respectively.

(v) The results suggest that the adopted strategy addressed the poor mechanical properties of the SPS-ed WC, so that the fabricated cermet parts can be used in various industrial applications, such as cutting and mining tools. For applications requiring highest toughness and strength, WC-18Co is recommended, whereas WC-1Cr offers a better balance of retained hardness and improved wear resistance.

Declaration of generative AI and AI-assisted technologies

The author(s) declare that no generative AI or AI-assisted technologies were used in the writing process of this manuscript.

[DOI: 10.22068/ijmse.4597]

Declaration of Interest

The authors declare that they have no known competing financial interests or personal relationships that could have appeared to influence the work reported in this paper.

References

[1] Yamanoglu R., "*Pressureless spark plasma sintering: A perspective from conventional sintering to accelerated sintering without pressure.*" *Powder Metallurgy and Metal Ceramics.* 2019, 57, 513-525.

[2] Zhang W, Yamashita S, and Kita H., "*Progress in pressureless sintering of boron carbide ceramics–a review.*" *Advances in Applied Ceramics.* 2019, 118(4), 222-239.

[3] Snetkov I.L., Zhou D, Yakovlev A.I., Volkov M.R., Kuznetsov I.I., Mukhin I.B., Palashov O.V., Shi Y, and Ueda K.I., "*Laser generation on Yb: LuAG ceramics produced by nanocrystalline pressure-less sintering in H_2.*" *Laser Physics Letters.* 2018, 15(3), 035801.

[4] Gong Y, Tian W, Zhang P, Chen J, Zhang Y, and Sun Z., "*Slip casting and pressureless sintering of Ti_3AlC_2.*" *Journal of Advanced Ceramics.* 2019, 8, 367-376.

[5] Zhu D, Zhou J, Huo T, Zheng J, Dai Y, Wu J., "*Fabrication of high transmittance AlON ceramics by three-step pressureless sintering.*" *Journal of Materials Research and Technology.* 2024, 33, 8992-9000.

[6] Chuvildeev V.N., Panov D.V., Boldin M.S., Nokhrin A.V., Blagoveshchensky Y.V., Sakharov N.V., Shotin S.V., and Kotkov D.N., "*Structure and properties of advanced materials obtained by Spark Plasma Sintering.*" *Acta Astronautica.* 2015, 109, 172-176.

[7] Zhang Z.H., Liu Z.F., Lu J.F., Shen X.B., Wang F.C., Wang Y.D., "*The sintering mechanism in spark plasma sintering–proof of the occurrence of spark discharge.*" *Scripta Materialia.* 2014, 81, 56-59.

[8] Deng S, Zhao H, Li R, Yuan T, Li L, Cao P., "*The influence of the local effect of electric current on densification of tungsten powder during spark plasma sintering.*" *Powder Technology.* 2019, 356, 769-777.

[9] Lee G, Manière C, McKittrick J, Doerner R, Nishijima D, Gattuso A, Abrams T, Thomas D, Back C, Olevsky EA. "*Consolidation of Molybdenum nanopowders by spark plasma sintering: Densification mechanism and first mirror application.*" *Journal of Nuclear Materials*. 2019, 516, 354-359.

[DOI: 10.22068/ijmse.4597]

[10] Tokita M., "*Progress of spark plasma sintering (SPS) method, systems, ceramics applications and industrialization.*" *Ceramics.* 2021, 4(2), 160-198.

[11] Azarniya A, Azarniya A, Safavi M.S., Farshbaf Ahmadipour M, Esmaeeli Seraji M, Sovizi S, Saqaei M, Yamanoglu R, Soltaninejad M, Madaah Hosseini H.R., Ramakrishna S., "*Physicomechanical properties of porous materials by spark plasma sintering.*" *Critical Reviews in Solid State and Materials Sciences.* 2020, 45(1), 22-65.

[12] Azarniya A, Safavi MS, Sovizi S, Azarniya A, Chen B, Madaah Hosseini HR, Ramakrishna S., "*Metallurgical challenges in carbon nanotube-reinforced metal matrix nanocomposites.*" *Metals.* 2017, 7(10), 384.

[13] Buravlev I.Y., Shichalin O.O., Belov A.A., Marmaza P.A., Kolodeznikov E.S., Dvornik M.I., Sakhnevich A.N., Buravleva A.A., Chuklinov S.V., Papynov E.K., "*Microstructural evolution and mechanical behavior of WC–4wt.% TiC–3wt.% TaC–12wt.% Co refractory cermet consolidated by spark plasma sintering of mechanically activated powder mixtures.*" *Advanced Powder Technology.* 2024, 35(10), 104625.

[14] Pramanik S, Srivastav A.K., Jolly B.M., Chawake N, Murty B.S., "*Effect of Re on microstructural evolution and densification kinetics during spark plasma sintering of nanocrystalline W.*" *Advanced Powder Technology.* 2019, 30(11), 2779-2786.

[15] Xiao Y, Peng X, Fu T., "*A novel high-entropy alloy with multi-scale precipitates and excellent mechanical properties fabricated by spark plasma sintering.*" *Advanced Powder Technology*. 2022, 33(3), 103520.

[16] Guan H.D., Li C.J., Gao P, Yi J.H., Bao R, Tao J.M., Fang D, Feng Z.X., "*Fe-based metallic glass particles reinforced Al-7075 matrix composites prepared by spark plasma sintering.*" *Advanced Powder Technology*. 2020, 31(8), 3500-3506.

[17] Fang Z.Z., Wang X, Ryu T, Hwang K.S., Sohn H.Y., "*Synthesis, sintering, and mechanical properties of nanocrystalline cemented tungsten carbide–a review.*" *International Journal of Refractory Metals and Hard Materials.* 2009, 27(2), 288-299.

[18] Sun J, Zhao J, Huang Z, Yan K, Shen X, Xing J, Gao Y, Jian Y, Yang H, Li B., "*A review on binderless tungsten carbide: development and application.*" *Nano-micro letters.* 2020, 12, 1-37.

[19] Lunk H.J., Hartl H., "*Discovery, properties and applications of tungsten and its inorganic compounds.*" *ChemTexts*. 2019, 5(3),15.

[20] Zhang J, Saeed M.H., Li S., "*Recent progress in development of high-performance tungsten carbide-based composites: Synthesis, characterization, and potential applications.*" *Advances in Ceramic Matrix Composites.* 2018, 307-329.

[21] Tripathy H, Sudha C, Paul V.T., Thirumurugesan R, Prasanthi T.N., Sundar R, Vijayashanthi N, Parameswaran P, Raju S., "*High temperature thermophysical properties of spark plasma*

[DOI: 10.22068/ijmse.4597]

sintered tungsten carbide." *International Journal of Refractory Metals and Hard Materials.* 2022, 104, 105804.

[22] Qu H, Zhu S, Li Q, Ouyang C., "*Influence of sintering temperature and holding time on the densification, phase transformation, microstructure and properties of hot pressing WC–40 vol.% Al_2O_3 composites.*" *Ceramics International*. 2012, 38(2), 1371-1380.

[23] Katiyar P.K., Singh P.K., Singh R, Lava Kumar A., "*Modes of failure of cemented tungsten carbide tool bits (WC/Co): A study of wear parts.*" *International Journal of Refractory Metals and Hard Materials.* 2016, 54, 27-38.

[24] Liu Y.X., Niu Y.B.., Lin N, Lu P, Wu ZG., Ma C., "*Microstructural stability and properties of tungsten-containing high-entropy carbonitride ceramic-based cermets.*" *Ceramics International.* 2025, 51, 36585-36592.

[25] Pirmohammadi P, Zakeri M, Razavi M, Nikzad L., "*Effect of SPS frequency on the transformation of diamond to graphite in WC-Co composite.*" *International Journal of Refractory Metals and Hard Materials.* 2024, 119, 106496.

[26] Niu Y, Gong P, Xu X, Wang X, Ma Y, Li M, Lu Q, Yang H, Liu Z, Zhang M, Tang X., "*Preparation of WC-Co cemented carbide by spark plasma sintering: Microstructure evolution, mechanical properties and densification mechanism.*" *International Journal of Refractory Metals and Hard Materials.* 2025, 126, 106964.

[27] Shichalin O.O., Buravlev I.Y., Portnyagin A.S., Dvornik M.I., Mikhailenko E.A., Golub A.V., Zakharenko A.M., Sukhorada A.E., Talskikh K.Y.., Buravleva AA., Fedorets A.N., "*SPS hard metal alloy WC-8Ni-8Fe fabrication based on mechanochemical synthetic tungsten carbide powder.*" *Journal of Alloys and Compounds*. 2020, 816, 152547.

[28] Verma V, Kumar B.M., "*Sliding wear behavior of SPS processed TaC-containing Ti (CN)-WC-Ni/Co cermets against Silicon Carbide*." *Wear*. 2017, 376, 1570-1579.

[29] Pan Y, Liu A, Huang L, Du Y, Jin Y, Yang X, Zhang J., "*Effects of metal binder content and carbide grain size on the microstructure and properties of SPS manufactured WC–Fe composites*." *Journal of Alloys and Compounds*. 2019, 784, 519-526.

[30] Zhang Z, Ning J, Ge M, Wu K, Liao H, Sun X, Wu D., "*Effect of W-to-C atomic ratio on microstructure and performance of in-situ WC/Fe composite prepared by spark plasma sintering*." *International Journal of Refractory Metals and Hard Materials*. 2024, 121, 106643.

[31] Eatemadi R, Balak Z., "*Investigating the effect of SPS parameters on densification and fracture toughness of ZrB2-SiC nanocomposite*." *Ceramics International*. 2019, 45(4), 4763-4770.

[32] Shamanian M, Mirzaei A, Kangazian J, Szpunar J.A., "*Characterization and mechanical behavior of AISI 316L/Incoloy 825 dissimilar welds processed by friction stir welding*." *Journal of Manufacturing Processes*. 2020, 55, 66-77.

[DOI: 10.22068/ijmse.4597]

[33] Liu K, Wang Z, Yin Z, Cao L, Yuan J., "*Effect of Co content on microstructure and mechanical properties of ultrafine grained WC-Co cemented carbide sintered by spark plasma sintering*." *Ceramics International*. 2018, 44(15), 18711-8.

[34] Xiao M.D., Xiao W, Jiang J.L., "*Cobalt phase structure of cemented carbide*." *Mater. Sci. Eng. Powder Metall.* 2010, 15, 611-614.

[35] Park C, Kim J, Kang S., "*Effect of cobalt on the synthesis and sintering of WC-Co composite powders*." *Journal of Alloys and Compounds*. 2018, 766, 564-571.

[36] Wang X, Fang Z.Z., Sohn H.Y., "*Grain growth during the early stage of sintering of nanosized WC–Co powder.*" *International Journal of Refractory Metals and Hard Materials*. 2008, 26(3), 232-241.

[37] Kumar A, Singh K, Pandey O.P., "*Sintering behavior of nanostructured WC–Co composite*." *Ceramics International*. 2011, 37(4),1415-1422.

[38] Oliver C.G., Alvarez E.A., García J.L., "*Kinetics of densification and grain growth in ultrafine WC-Co composites.*" *International Journal of Refractory Metals and Hard Materials*. 2016, 59, 121-131.

[39] Armstrong R.W., "*The hardness and strength properties of WC-Co composites*." *Materials*. 2011, 4(7), 1287-1308.

[40] Pittari III J.J, Swab J.J., Wright J, Atwater K., "*Mechanical evaluation of WC-Co materials with varying microstructures*." *International Journal of Refractory Metals and Hard Materials*. 2022, 104,105809.

[41] Safavi M.S., Walsh F.C., "*The electrodeposition of particle-metal matrix composite coatings to meet tribological and corrosion challenges*." *Advances in Colloid and Interface Science*. 2025, 343:103584.

[DOI: 10.22068/ijmse.4597]